energies

MDPI

Article

Experimental Investigation of Free Convection Heat Transfer from Horizontal Cylinder to Nanofluids

Dorota Sawicka [1], Janusz T. Cieśliński [2,*] and Slawomir Smolen [1]

[1] Faculty of Nature and Engineering, J.R. Mayer–Institute for Energy Engineering, City University of Applied Sciences Bremen, Neustadtswall 30, 28199 Bremen, Germany; dorota.czerwonka@gmail.com (D.S.); Slawomir.Smolen@hs-bremen.de (S.S.)

[2] Faculty of Mechanical and Ship Technology, Institute of Energy, Gdańsk University of Technology, Narutowicza 11/12, 80233 Gdansk, Poland

* Correspondence: jcieslin@pg.edu.pl

Abstract: The results of free convection heat transfer investigation from a horizontal, uniformly heated tube immersed in a nanofluid are presented. Experiments were performed with five base fluids, i.e., ethylene glycol (EG), distilled water (W) and the mixtures of EG and water with the ratios of 60/40, 50/50, 40/60 by volume, so the Rayleigh (Ra) number range was $3 \times 10^4 \leq \mathrm{Ra} \leq 1.3 \times 10^6$ and the Prandtl (Pr) number varied from 4.4 to 176. Alumina (Al_2O_3) nanoparticles were tested at the mass concentrations of 0.01, 0.1 and 1%. Enhancement as well as deterioration of heat transfer performance compared to the base fluids were detected depending on the composition of the nanofluid. Based on the experimental results obtained, a correlation equation that describes the dependence of the average Nusselt (Nu) number on the Ra number, Pr number and concentration of nanoparticles is proposed.

Keywords: free convection; horizontal cylinder; nanofluids; correlation equation

Citation: Sawicka, D.; Cieśliński, J.T.; Smolen, S. Experimental Investigation of Free Convection Heat Transfer from Horizontal Cylinder to Nanofluids. *Energies* **2021**, *14*, 2909. https://doi.org/10.3390/en14102909

Academic Editor: Jose A. Almendros-Ibanez

Received: 29 March 2021
Accepted: 10 May 2021
Published: 18 May 2021

1. Introduction

Nanofluids have come to be seen as a new generation of coolants, both in single-phase and two-phase systems, e.g., [1–4]. Furthermore, nanofluids or nanocomposites may be used as a medium in thermal energy storage systems as sensible heat storage [5] and phase change materials [6]. In sensible heat storage systems, the dominating mechanism of the heat transfer is free convection. Contrary to forced convection [7,8], not many studies dealing with the free convection of nanofluids exist today. Moreover, the greater part of them are devoted to the free convection of nanofluids in enclosures of different, sometimes very sophisticated, geometries and thermal conditions. A comprehensive review of free convection of nanofluids in cavities is presented in [9].

Relatively few experimental studies have been carried out on free convection around bodies immersed in nanofluids. Cieśliński and Krygier [10] experimentally established the deterioration of heat transfer during the free convection of water–Al_2O_3 nanofluid with 0.01% nanoparticle concentration by weight from a horizontal, electrically heated tube covered with a metallic porous coating. Kiran and Babu [11] experimentally studied free convection heat transfer using transformer oil–TiO_2 nanofluids with various volume concentrations from 0.05 to 0.2%, as the tested element served as an electrically heated vertical cylinder. It was observed that the addition of nanoparticles up to 0.15% improves heat transfer. For higher concentrations of TiO_2 nanoparticles, degradation of heat transfer was observed. The unique, closely related theoretical study to the present paper is the work by Habibi et al. [12]. Habibi et al. analytically solved the problem of free convection from a horizontal cylinder immersed in an unbounded water–Al_2O_3 nanofluid. Nanoparticle concentration by volume ranged from 0 to 10%. It was established that the decisive parameter influencing fluid motion and heat transfer around the horizontal cylinder is

viscosity. Following Polidori et al. [13], two formulas were tested: Brinkman model [14] and the Maïga et al. correlation [15]. Results of the calculations show that application of the Brinkman model of nanofluid viscosity leads to a moderate increase in the Nu number with increasing nanoparticle concentration (up to 20%). Contradictory results were obtained using the Maïga et al. correlation. In this case, a distinct decrease in Nu number with nanoparticle increase was detected. Building on the results of the parametric study, two correlations (based on the Brinkman model and Maïga et al. correlation nanofluid viscosity formulas) are proposed for the average Nu number of the alumina–water nanofluid in terms of Ra number and nanoparticle concentration.

As seen in the presented literature review, there is a lack of experimental study dealing with free convection heat transfer from a horizontal cylinder immersed in an unbounded nanofluid. Geometry of the experimental container was designed such that the generated motion of the fluid was not significantly affected by the free surface of the liquid, side walls and bottom surface. In order to avoid influence of axial conduction on heat transferred from the cylinder, the length-to-diameter ratio was made to be large. In the present work, the results of free convection heat transfer performance from a uniformly heated horizontal tube are discussed. Base fluids are ethylene glycol (EG), water (W) and mixtures of EG and water at the ratios 60/40, 50/50 and 40/60 by volume. Alumina (Al_2O_3) nanoparticles were tested at the mass concentrations of 0.01, 0.1 and 1%.

2. Experimental Setup

2.1. Experimental Apparatus

The main parts of the experimental stand were the test container, horizontal tube, power system, DAQ-module and LabVIEW-based data measuring and data processing system. The test container made of PMMA had inner dimensions of 160 × 160 × 500 mm—Figure 1.

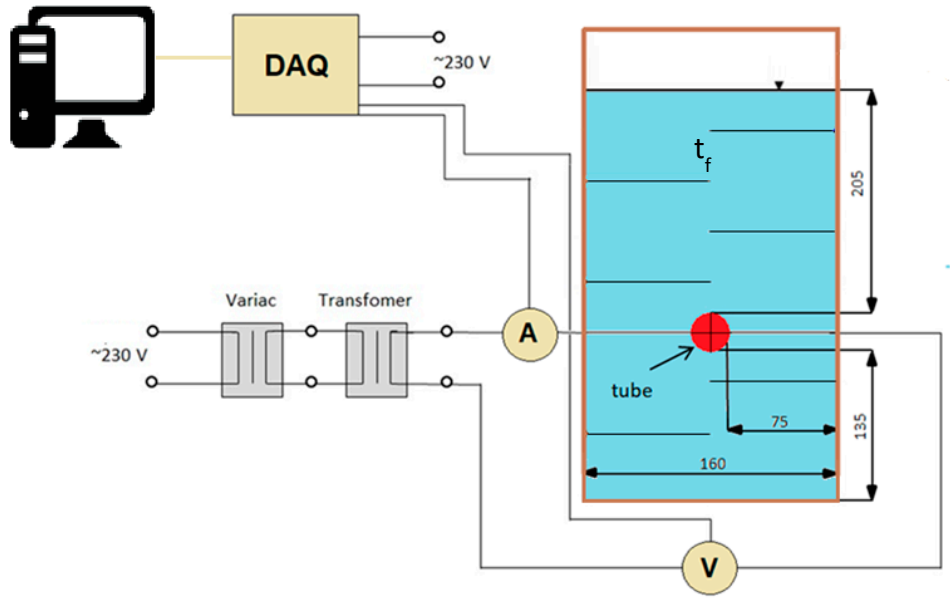

Figure 1. Scheme of the experimental setup.

The container is thermally insulated with Styrodur. In order to fulfil the condition of free convection in an unbounded nanofluid, the geometry of the tested thermal system was carefully designed. The confinement ratios are as follows: $H_T/D = 20.5$, $H_B/D = 13.5$ and $S_W/D = 7.5$. The details of the thermal system are discussed in [16]. Twelve resistance thermometers of type Pt100 and tolerance class B were used to measure liquid temperature. The resistance thermometers were produced by TC Direct (Mönchengladbach, Germany). A stainless steel tube with OD of 10 and 0.6 mm wall thickness was used as a test heater.

With L = 15 D, the tube was long enough to neglect influence of side walls on heat transfer [17–19]. The tube was heated by Joule heat. Two resistance thermometers Pt100 were used to measure inside temperature of the heating tube. Power supply was adjusted by a panel of two auto-transformers—Figure 1. Data recording and management was done using a Texas Instruments DAQ-module and LabVIEW 2015 (National Instruments, Austin, TX, USA). Experiments were conducted under steady state conditions. Steady state was assumed to have been reached when the temperature difference between the cylinder's wall and liquid was less than 0.1 K [20]. A successive steady state was established by increasing the current to the heating section. A new steady state was reached after 15–20 min. Maximum electrical power supplied to the tube was 120 W ($q \approx 20$ kW/m^2).

2.2. Nanofluid Preparation

The tested fluids were ethylene glycol, distilled water and mixtures of ethylene glycol-distilled water (60/40), (50/50) and (40/60) by volume. For the nanoparticles, alumina (Al_2O_3) was used. The nanoparticles had a spherical form and their diameter was in a range from 5 to 250 nm, while their mean diameter was 47 nm according to the manufacturer Sigma Aldrich Ltd. (Munich, Germany). The nanofluids were tested at nanoparticle mass concentrations of 0.01, 0.1 and 1%. The nanofluids were prepared with the two-step method. The first step was the preparation of the concentrated nanofluid in laboratory glasses of 250 mL. Then, the nanoparticles were suspended in a base fluid and put into an ultrasonic bath for 1 h. The ultrasonic washer Elmasonic S180H from Elma Schmidbauer GmbH (Singen, Germany) worked at a frequency of 37 Hz and effective power of 200 W. Next, the concentrated nanofluids were mixed with the rest of the base fluid until the volume of 10 L was prepared. Finally, the fluid was homogenized with a high-speed homogenizer X1740 from CAT GmbH (Tübingen, Germany) with a speed of rotation of 12,000 rpm for 1 h. As an example, Figure 2 shows photographs of the tested ethylene glycol-based nanofluids.

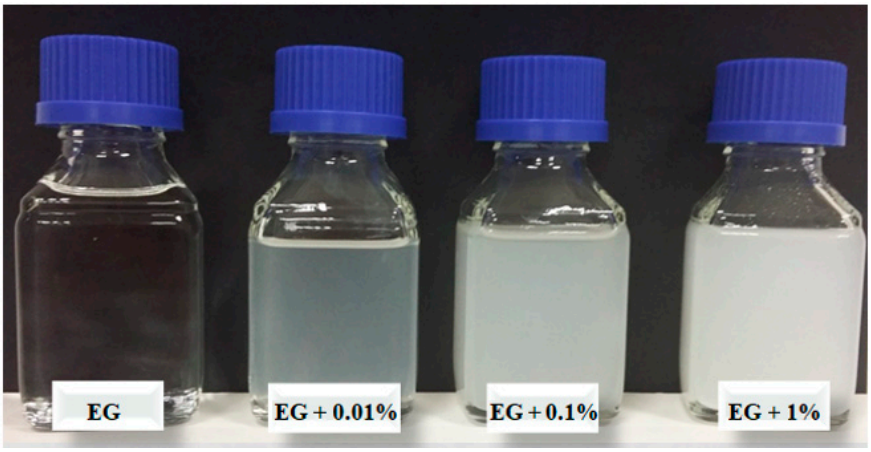

Figure 2. Tested EG–Al_2O_3 nanofluids.

2.3. Nanofluid Properties

The literature results show a key role of the effective thermal conductivity and the effective viscosity of nanofluids in free convection heat transfer. Therefore, in order to avoid ambiguity in the interpretation of the present results, the thermal conductivity and the viscosity of the tested nanofluids were determined experimentally [21]. The developed present correlations for the thermal conductivity and the effective viscosity of the tested nanofluids are listed in Tables 1 and 2, respectively.

Table 1. Correlations for the thermal conductivity of the tested nanofluids.

Liquid	Correlation	Equation Number
Water	$k_{nf} = k_{bf}(1 + 0.1046\varphi_m{}^{0.2388}\ (100/d_p)^{3.14\cdot10^{-3}})$	Equation (1)
EG	$k_{nf} = k_{bf}(1 + 0.0193\left(\frac{k_p}{k_{bf}}\right)^{6.15\cdot10^{-3}}\varphi_m{}^{0.0738}\ (100/d_p)^{9.76\cdot10^{-5}})$	Equation (2)
Water/EG (60:40)	$k_{nf} = k_{bf} = 1.428\cdot10^{-3}T$	Equation (3)
Water/EG (50:50)	$k_{nf} = k_{bf} = 1.334\cdot10^{-3}T$	Equation (4)
Water/EG (40:60)	$k_{nf} = k_{bf} = 1.166\cdot10^{-3}T$	Equation (5)

Table 2. Correlations for the dynamic viscosity of the tested nanofluids.

Liquid	Correlation	Equation Number
Water	$\mu_{nf} = 664.06\varphi_m{}^{0.0151}t^{0.0236}\mu_{bf}^{1.939}$	Equation (6)
EG	$\mu_{nf} = 1.11\varphi_m{}^{0.0061}\mu_{bf}^{1.017}$	Equation (7)
Water/EG (60:40)	$\mu_{nf} = 1.13\varphi_m{}^{0.0106}\mu_{bf}^{1.003}$	Equation (8)
Water/EG (50:50)	$\mu_{nf} = 1.14\mu_{bf}^{0.9906}$	Equation (9)
Water/EG (40:60)	$\mu_{nf} = 2.83\varphi_m{}^{0.0094}t^{0.279}\mu_{bf}^{1.3237}$	Equation (10)

Density and specific heat of the tested nanofluids were determined by use of the Equations (11) and (12) proposed by Pak and Cho [22], respectively

$$\rho_{nf} = \varphi_v\rho_p + (1 - \varphi_v)\rho_{bf} \tag{11}$$

$$c_{p,nf} = \varphi_v c_{p,p} + (1 - \varphi_v)c_{p,bf} \tag{12}$$

The thermal expansion coefficient was determined from the equation proposed by Khanafer et al. [23]

$$\beta_{nf} = \frac{(1 - \varphi_v)\beta_{bf}\rho_{bf} + \varphi_v\rho_p\beta_p}{\rho_{nf}} \tag{13}$$

Thermophysical properties of the base fluids were obtained from the data provided in the ASHRAE Handbook [24]. The appropriate correlations are shown in Table 3.

Table 3. Correlations for the thermophysical properties of the base fluids.

Parameter	Water	EG
Thermal conductivity [W/(mK)]	$k_{bf} = 1.974\cdot10^{-3}\cdot T$	$k_{bf} = 8.49\cdot10^{-4}\cdot T$
Viscosity [Pa s]	$\mu_{bf} = 1.435\cdot10^{-5}\cdot e^{\frac{1226.8}{T}}$	$\mu_{bf} = 1.6\cdot10^{-7}\cdot e^{\frac{3440}{T}}$
Density [kg/m^3]	$\rho_{bf} = 1107.6 - 0.3708\cdot T$	$\rho_{bf} = 1331.2 - 0.732\cdot T$
Specific heat [J/(kgK)]	$c_{pbf} = 5603 - 9.2129\cdot T + 0.0149\cdot T^2$	$c_{pbf} = 1062.3 + 4.507\cdot T$
Thermal expansion coefficient [1/K]	$\beta_{bf} = \left(9.3158\cdot10^{-3}t - \frac{4.7211}{t^2}\right)\cdot10^{-3}$	$\beta_{bf} = 0.00065$

The properties of alumina (Al_2O_3) nanoparticles are shown in Table 4.

Table 4. Properties of Al_2O_3 nanoparticles.

Thermal Conductivity [25] k_p [W/(mK)]	Density [26] ρ_p [kg/m^3]	Specific Heat [26] c_{pp} [J/(kg K)]	Thermal Expansion Coefficient [27] β_p [1/K]
35	3600	765	8.46×10^{-6}

2.4. Stability of the Tested Nanofluids

Stability of the nanofluids is a critical factor in the application of nanofluids that can alter not only the thermo-physical properties of nanofluids but also the thermal character-

istics of the heating surface [28–30]. For this study, the stability of the tested nanofluids was estimated by the turbidity measurement using WTW device Turb 430 IR from Xylem—WTW (Weilheim in Oberbayern, Bavaria, Germany). The measurement principle of this device is based on the spectrophotometry method. The nephelometric turbidity units (NTUs) were recorded and found to be slightly changed over the period of performed testing—a period exceeding 14 days. A single NTU value of the turbidity was calculated as an average of three measurements. Figure 3 shows the turbidity of EG-based nanofluids as a function of time. For these nanofluids, the turbidity was measured for a period of 11 to 13 days. It was found that the stability of the tested EG-based nanofluids is satisfactory for the tested period. After 13 days, the maximum turbidity change of 26% was observed for the nanoparticle concentration of 0.01%.

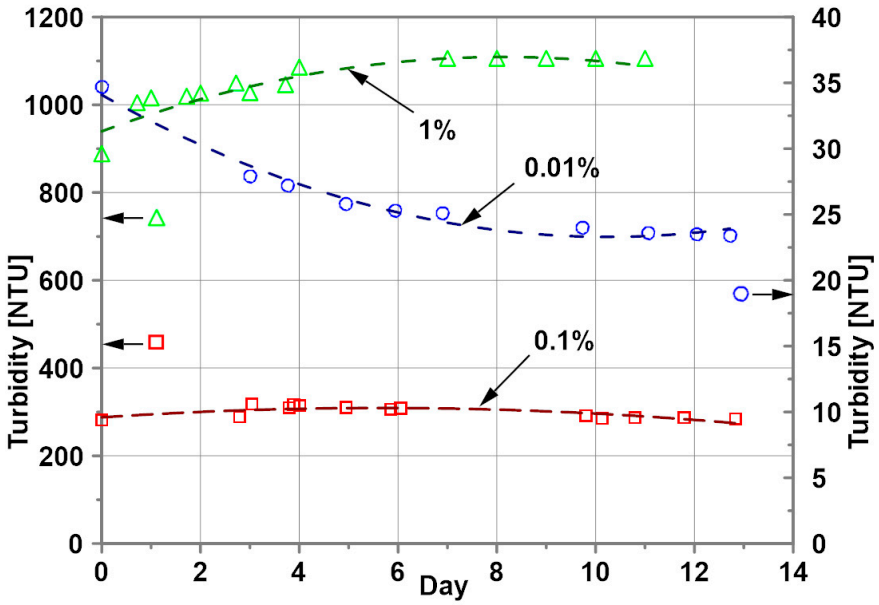

Figure 3. Turbidity of EG–Al_2O_3 nanofluids; nanoparticle concentration: ○ - 0.01%, □ - 0.1%, △ - 1%.

The change in water-based nanofluids' turbidity is substantial for lower nanoparticle concentrations (Figure 4). The turbidity decreased during the first 3 days by 73 and 72% for nanoparticle mass concentrations of 0.1 and 0.01%, respectively, a decrease in the turbidity results from the sedimentation process. Surprisingly, the turbidity of the nanofluid with 1% nanoparticle concentration is almost constant over the period of 7 days.

2.5. Data Reduction and Measurement Uncertainty

The algorithm of the data reduction as well as the procedure of measurement uncertainty estimation were the same as in the case presented in [16]. According to the calculations shown in [16], the maximum errors for the heat flux and heat transfer coefficient were estimated to be ±4.2 and ±5.5%, respectively.

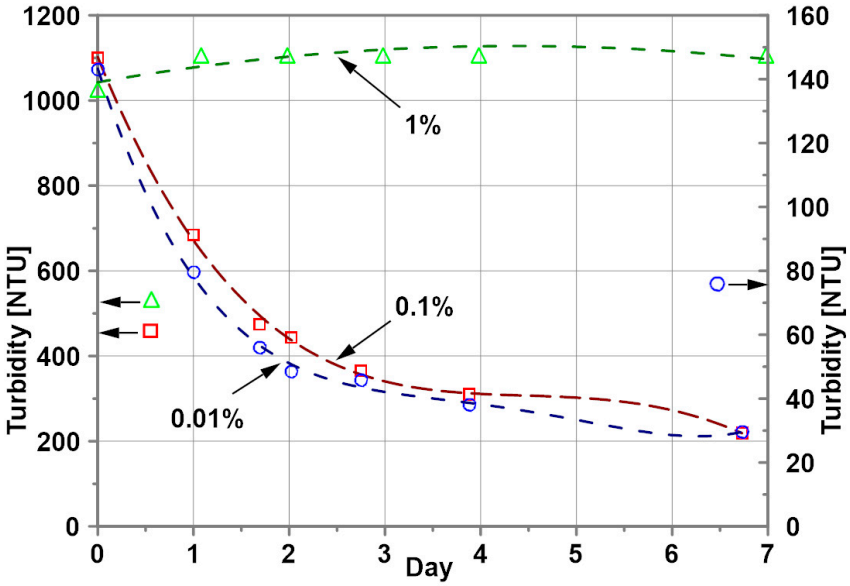

Figure 4. Turbidity of water–Al_2O_3 nanofluids; nanoparticle concentration: ○ - 0.01%, □ - 0.1%, △ - 1%.

3. Results

3.1. Validation of the Research Methods

A number of experimental tests using base fluids, i.e., water, EG and water/EG mixtures, were conducted in order to validate the present experimental setup and procedure. The present experimental results are compared with the recognized Churchill and Chu correlation recommended for uniformly heated, isolated horizontal cylinders immersed in unbounded fluid [31].

$$\mathrm{Nu} = \left(0.6 + \frac{0.387(\mathrm{Ra_q}/\mathrm{Nu})^{1/6}}{\left[1 + \left(\frac{0.559}{\mathrm{Pr}}\right)^{\frac{9}{16}}\right]^{\frac{8}{27}}} \right)^2 \tag{14}$$

As an example, Figure 5 shows comparison of the predictions from the present developed empirical correlation for water [16]

$$\mathrm{Nu} = 0.4017\ \mathrm{Ra_q^{0.2109}Pr^{0.166}} \tag{15}$$

and the predictions obtained from the Churchill and Chu correlation (Equation (14)). The Churchill and Chu correlation underestimates predictions from the developed Equation (15) with a satisfactory maximum deviation of 3.4%.

3.2. Influence of Nanoparticle Concentration on Heat Transfer

The experimental investigation on EG-based nanofluids was performed for heat flux from 2000 to 14,000 W/m^2. The corresponding temperature difference ranged from 8 to 38 K.

Experimental results (Figure 6) revealed that the addition of nanoparticles results in an increase or decrease in the Nu numbers depending on nanoparticle concentration compared to pure EG. A slight increase in Nu number was recorded for nanoparticle mass concentration of 0.1%. For the nanoparticle concentrations of 0.01 and 1%, a decrease in Nu number was noted. The highest decrease in the Nu number was observed for the nanoparticle concentration of 1% and amounted 12% in comparison to pure EG. The red line in Figure 6 represents the developed empirical correlation for pure EG.

$$\mathrm{Nu} = 0.4673\ \mathrm{Ra^{0.231}Pr^{0.096}} \tag{16}$$

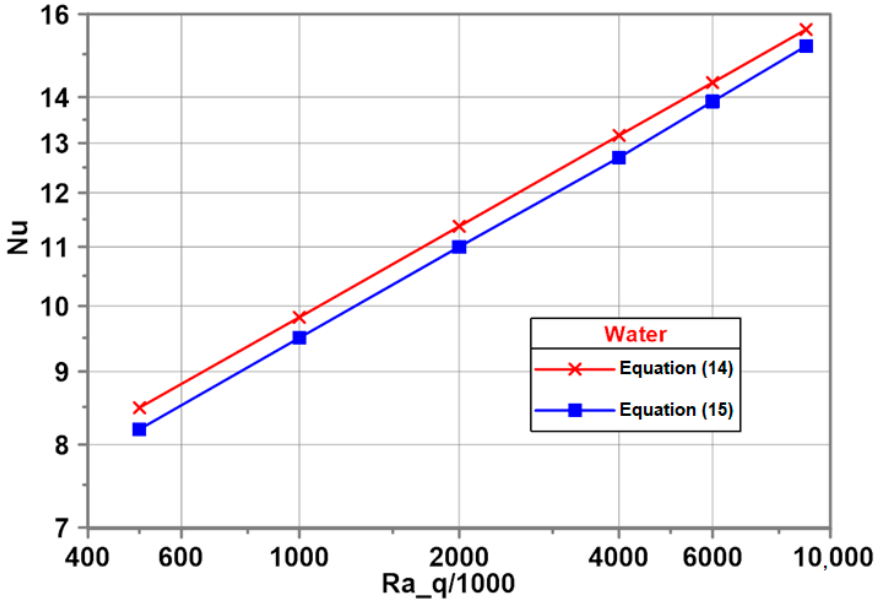

Figure 5. Present data compared to predictions from the literature correlation.

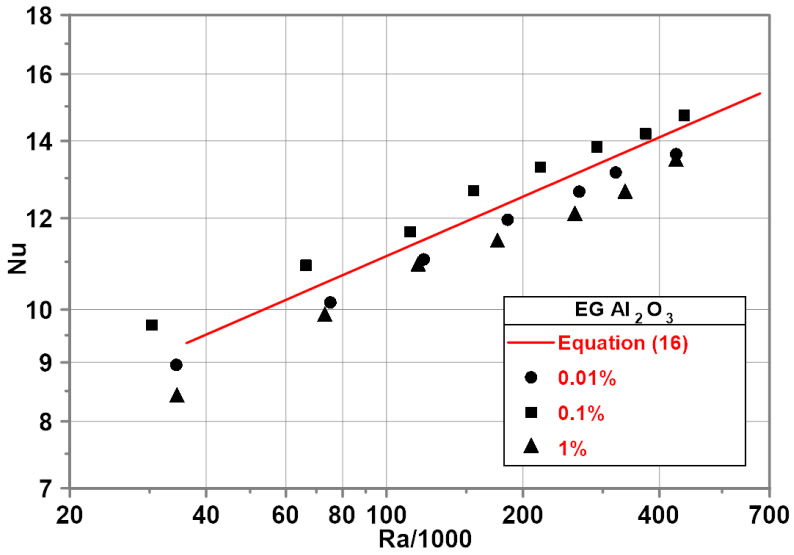

Figure 6. Nu–Ra relationship for ethylene glycol-based nanofluids.

An experimental investigation of water-based nanofluids has been performed for heat flux from 2000 to 22,000 W/m^2. The corresponding temperature difference ranged from 3 to 25 K.

Similar to the EG–Al_2O_3 (0.1%) nanofluid, the water–Al_2O_3 mixture with a nanoparticle mass concentration of 0.1% exhibits an increase in Nu number compared to pure water. The maximum increase in Nu number was about 7% for the minimum Ra number—Figure 7. A decrease in the Nu numbers was observed for the water–Al_2O_3 mixture with a nanoparticle mass concentration of 0.01% compared to pure water. No influence of nanoparticles on the Nu numbers was observed for the water–Al_2O_3 nanofluid with a nanoparticle mass concentration of 1%—the measurement points overlap the red line representing a developed empirical correlation for pure water.

$$\mathrm{Nu} = 0.374\,\mathrm{Ra}^{0.2613}\mathrm{Pr}^{0.16}. \quad (17)$$

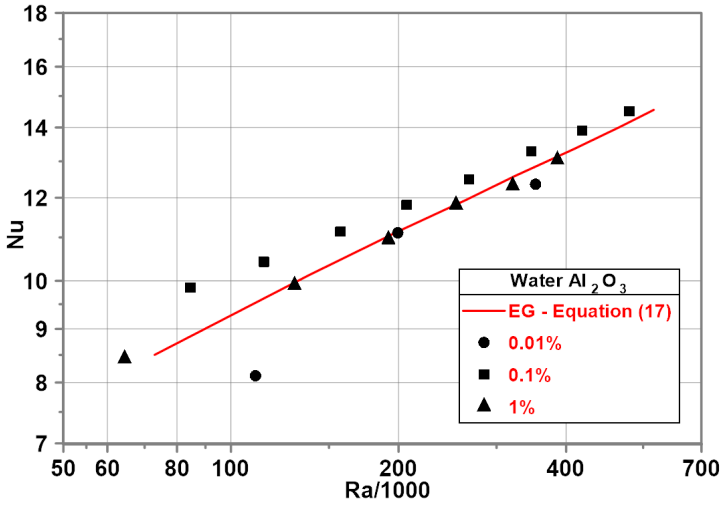

Figure 7. Nu–Ra relationship for water based nanofluids.

The experimental investigation of EG/water (60/40) mixture-based nanofluids was performed for heat flux from 2000 to 21,000 W/m^2. The corresponding temperature difference ranged from 4 to 35 K.

Experimental results show that the addition of nanoparticles with a mass concentration of 0.1% leads to an increase in the Nu numbers within the whole range of Ra numbers with a maximum of 15% for the minimum Ra number—Figure 8.

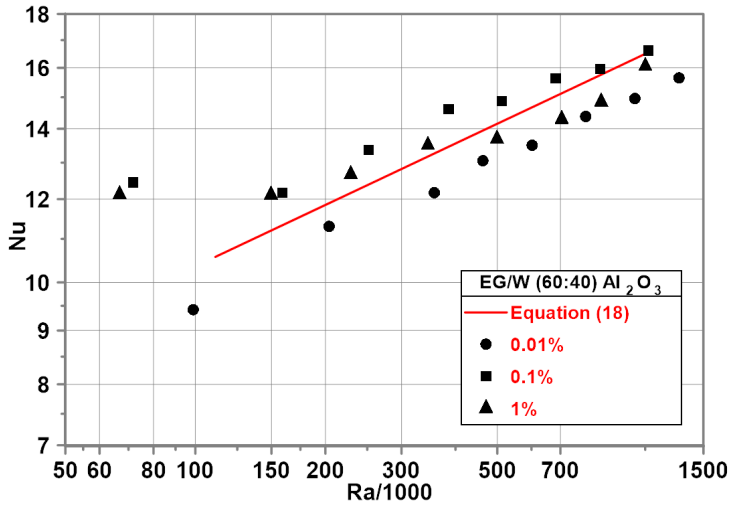

Figure 8. Nu–Ra relationship for EG/water (60/40) mixture-based nanofluids.

The red line in Figure 8 represents the developed empirical correlation for the EG/water (60/40) mixture.

$$\mathrm{Nu} = 1.110\mathrm{Ra}^{0.194} \quad (18)$$

A distinct decrease in the Nu numbers compared to the base fluid was noted for the nanofluid with 0.01% nanoparticle concentration with the average difference of about 8%. For the nanofluid with a nanoparticle mass concentration of 1%, the Nu numbers are higher than for the base fluid with Ra < 500,000. For higher Ra numbers, the Nu numbers are lower than for the base fluid with a maximum of 5% difference.

The experimental investigation of EG/water (50/50) mixture-based nanofluids was performed for heat flux from 2000 to 20,000 W/m^2. The corresponding temperature difference ranged from 4 to 30 K.

Experimental investigations show an increase in the Nu numbers within the whole range of the Ra number for the nanoparticle concentration of 0.01 and 0.1%—Figure 9. For

the nanoparticle mass concentration of 1%, a decrease in the Nu numbers in comparison to pure EG/water (50/50) mixture was observed with a maximum of 6% for the highest Ra number. The red line in Figure 9 represents the developed empirical correlation for the EG/water (50/50) mixture.

$$\mathrm{Nu} = 1.7053\ \mathrm{Ra}^{0.1626} \tag{19}$$

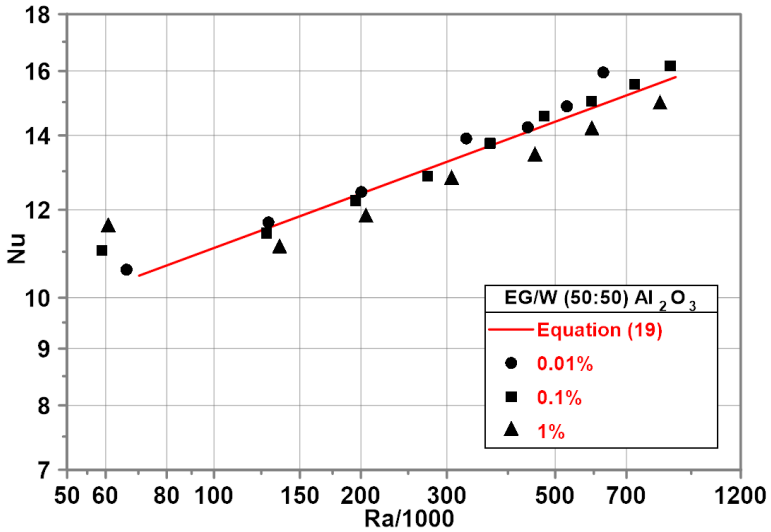

Figure 9. Nu–Ra relationship for EG/water (50/50)-based nanofluids.

The experimental investigation on EG/water (40/60) mixture-based nanofluids was performed for heat flux from 2000 to 22,000 W/m^2. The corresponding temperature difference ranged from 4 to 31 K.

Experimental results show an increase in the Nu numbers for the nanoparticle mass concentration of 0.1% within the whole range of the Ra numbers tested with a maximum of 5% for the maximum Ra number—Figure 10.

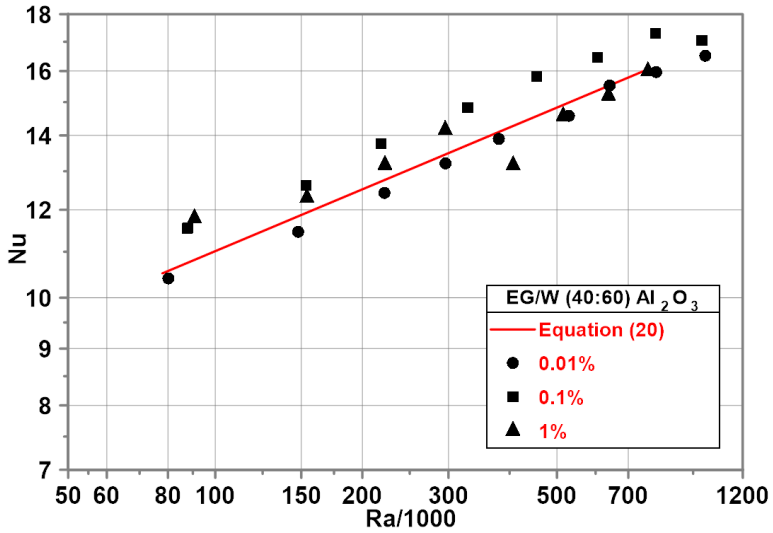

Figure 10. Nu–Ra relationship for EG/water (40/60)-based nanofluids.

The red line in Figure 10 represents the developed empirical correlation for the EG/water (40/60) mixture.

$$\mathrm{Nu} = 1.309\mathrm{Ra}^{0.185} \tag{20}$$

For the nanoparticle mass concentration of 0.01%, experimental points for the nanofluid almost overlap the data for a pure EG/water (40/60) mixture represented by the red line in

Figure 10. For the nanofluid with a nanoparticle mass concentration of 1%, the Nu numbers are higher than for the base fluid for Ra < 400,000. For higher Ra numbers, the Nu numbers are lower than for the base fluid.

Figure 11 illustrates the impact of nanoparticle concentration on the Nu numbers for water-based (Figure 11a) and EG-based (Figure 11b) nanofluids for selected heat fluxes. As expected, the Nu numbers increase with heat flux increase for all tested nanofluids. Experimental data show that independent on heat flux and base fluid, the Nu numbers reach a kind of optimum for the nanoparticle mass concentration of 0.1%.

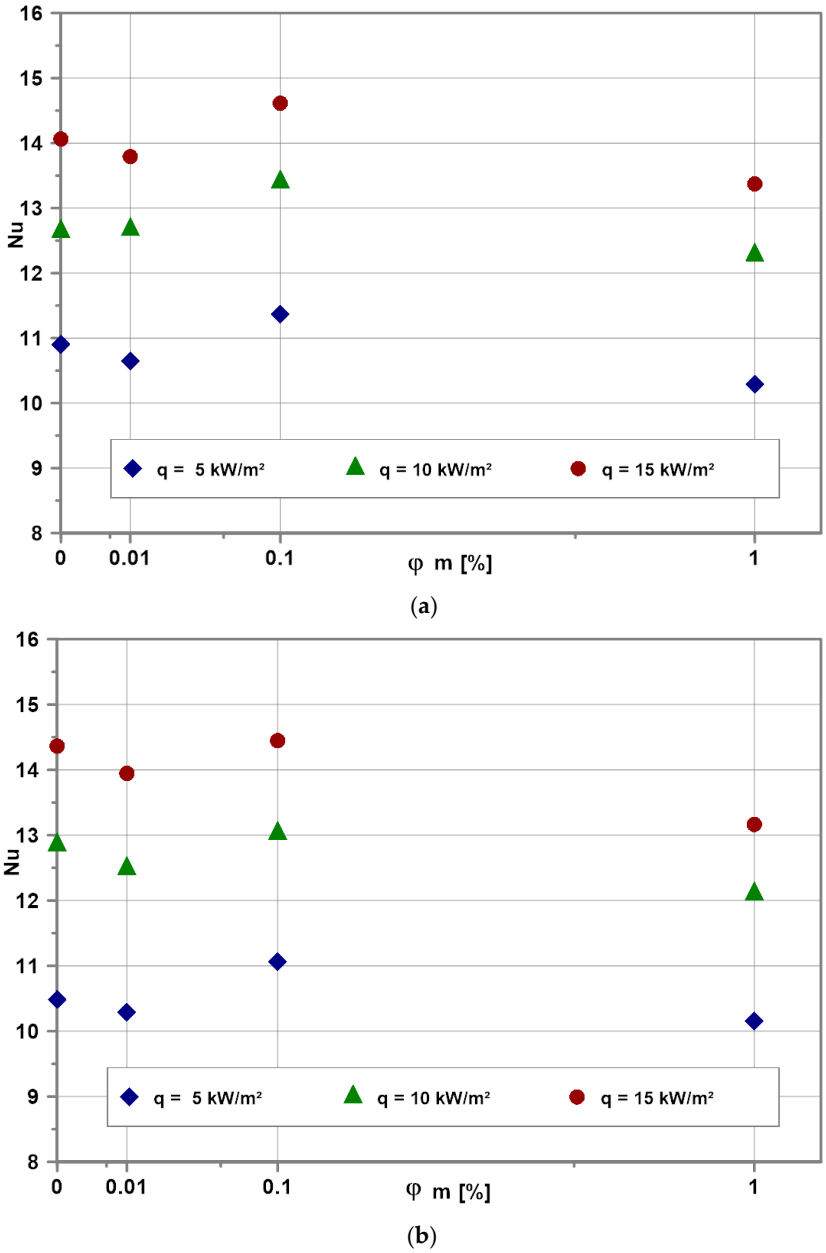

Figure 11. Influence of nanoparticle concentration on Nu number for selected heat fluxes for EG (**a**) and water (**b**).

3.3. Present Correlation

Putra et al. [32] correlated their experimental results of water-based nanofluids using an Nu-type correlation in the form $Nu = CRa^n$. However, as it was shown in [17], Nu number is a function of Ra number as well as Pr number. Xuan and Roetzel [33]

suggested that the correlation equation for nanofluids should include a concentration of the nanoparticles.

A multidimensional regression analysis based on the least squares method was used to develop a correlation equation for the Nu numbers for free convection of water–Al_2O_3, EG–Al_2O_3 and the mixtures of water and EG at the ratios of 60/40, 50/50, 40/60 by volume of nanofluids of different nanoparticle concentration from horizontal cylinder in an unbounded fluid.

$$\mathrm{Nu_{corr}} = 0.63\mathrm{Ra}^{0.23}\mathrm{Pr}^{0.053}(1-\varphi)^{2.64} \quad (21)$$

Figure 12 shows the comparison of the experimental results for all tested nanofluids with the predictions made from the developed correlation (Equation (21)). For 85% of points, the difference between experimental data and corresponding predictions is lower than ±10%. Considering the complexity of the examined process, the obtained agreement is satisfactory. The developed correlation is valid for the Ra number range $3 \times 10^4 \leq \mathrm{Ra} \leq 1.3 \times 10^6$, the Pr number range $4.4 < \mathrm{Pr} < 176$ and the mass concentrations of alumina nanoparticles $0.01\% \leq \varphi_m \leq 1\%$.

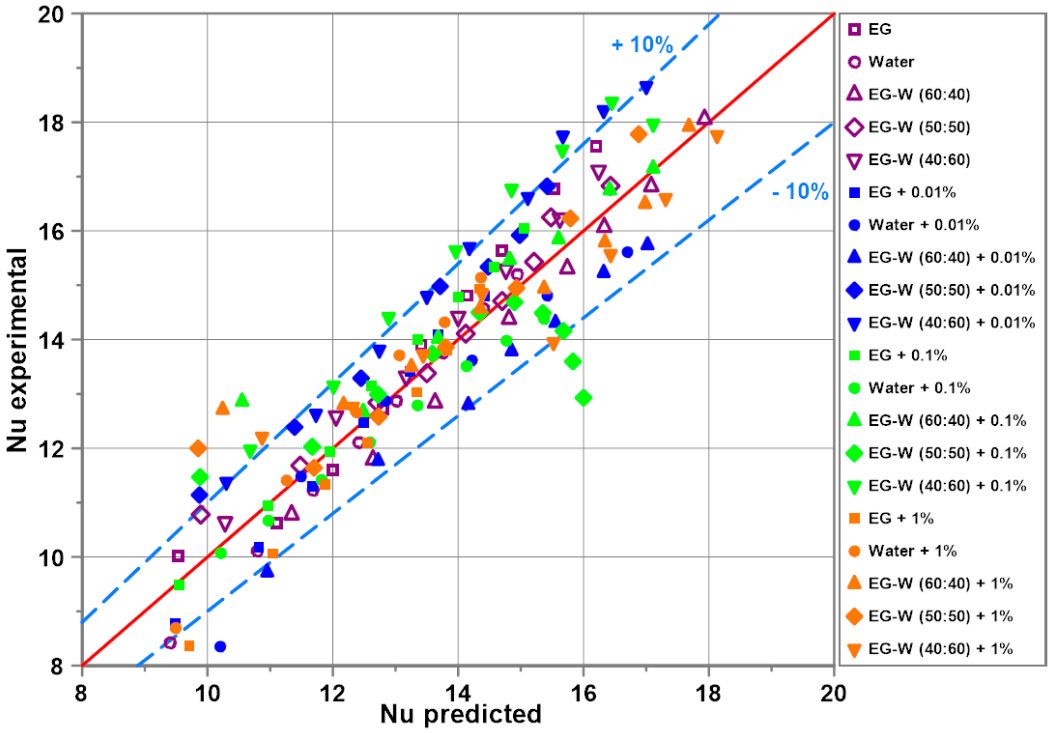

Figure 12. Experimental results vs. predictions from the developed correlation.

4. Discussion and Conclusions

Free convection heat transfer from a horizontal cylinder immersed in nanofluids was studied. The experimental setup was designed in order to fulfil requirements of free convection in an unbounded fluid.

In order to ensure wide range of Ra numbers, five base fluids were investigated, i.e., water, EG and water–EG mixtures: (60/40), (50/50) and (40/60) by volume. Alumina (Al_2O_3) nanoparticles were tested at the mass concentrations of 0.01, 0.1 and 1%.

Stability of the tested nanofluids as a fundamental issue of the potential application of the nanofluids was studied very carefully.

As it was established in [12,13,23,34], evaluation of the impact of nanoparticles on free convective heat transfer depends on the determination of the thermophysical properties of the analyzed nanofluids. Depending on the formulas adopted to calculate major properties, such as thermal conductivity and viscosity, contradictory results regarding the

influence of nanoparticles were found. Therefore, the present study's correlations for the calculation of thermal conductivity and viscosity of the tested nanofluids are based on actual measurements.

Present experimental data show that the addition of alumina nanoparticles to water, EG and mixtures of water and EG results in an increase or decrease in the Nu numbers depending on the nanoparticle concentration. An optimum of the Nu numbers was observed for the nanoparticle mass concentration of 0.1%.

A heat transfer correlation equation for the nanofluids has been developed and verified for various Ra numbers, Pr numbers and nanoparticle mass concentrations.

Author Contributions: Conceptualization, J.T.C.; methodology, J.T.C. and S.S.; software, D.S.; validation, J.T.C. and S.S.; formal analysis, J.T.C.; investigation, D.S.; data curation, D.S.; writing—original draft preparation, J.T.C.; writing—review and editing, J.T.C. and S.S.; funding acquisition, J.T.C. All authors have read and agreed to the published version of the manuscript.

Funding: This research received no external funding.

Institutional Review Board Statement: Not applicable.

Informed Consent Statement: Not applicable.

Acknowledgments: The authors thank Albrecht Eicke (City University of Applied Sciences Bremen) for kind cooperation during figures preparation.

Conflicts of Interest: The authors declare no conflict of interest.

Nomenclature

a	Thermal diffusivity	(m^2/s)
c_p	Specific heat	(J/(kg K))
D	Outer diameter of heated cylinder	(m)
g	Gravitational acceleration	(m/s^2)
h	Heat transfer coefficient	($W/(m^2$ K))
H_B	Distance between periphery of cylinder and bottom wall	(m)
H_T	Submersion depth	(m)
k	Thermal conductivity	(W/(m K))
$\boldsymbol{Nu}=\frac{hD}{k}$	Nu number	(-)
Pr	Pr number	(-)
$\boldsymbol{q}$	Heat flux	(W/m^2)
$\boldsymbol{Ra}=\frac{g\beta(T_w-T_f)D^3}{\nu a}$	Ra number related to temperature difference	(-)
$\boldsymbol{Ra_q}=\frac{g\beta qD^4}{k\nu a}$	Ra number related to heat flux	(-)
S_W	Distance between periphery of cylinder and side wall	(m)
t	Temperature	(°C)
T	Temperature	(K)
ΔT	Temperature difference	(K)
Greek Symbols		
$\boldsymbol{\beta}$	Thermal expansion coefficient	(1/K)
$\boldsymbol{\mu}$	Dynamic viscosity	(Pa s)
$\boldsymbol{\nu}$	Kinematic viscosity	(m^2/s)
$\boldsymbol{\varphi}$	Nanoparticle concentration	(-)
$\boldsymbol{\rho}$	Density	(kg/m^3)
Subscripts		
bf	Base fluid	
f	Fluid	
m	Mass	
nf	Nanofluid	
p	Particle	
v	Volume	
w	Wall	

References

1. Choi, S. Enhancing Thermal Conductivity of Fluids with Nanoparticles. In *Developments and Applications of Non-Newtonian Flows*; ASME: New York, NY, USA, 1995; Volume 231/MD, pp. 99–105.
2. Taylor, R.; Coulombe, S.; Otanicar, T.; Phelan, P.; Gunawan, A.; Lv, W.; Rosengarten, G.; Prasher, R.; Tyagi, H. Small particles, big impacts. A review of the diverse applications of nanofluids. *J. Appl. Phys.* **2013**, *113*, 011301. [CrossRef]
3. Sajid, M.U.; Ali, H.M. Recent advances in application of nanofluids in heat transfer devices: A critical review. *Renew. Sustain. Energy Rev.* **2019**, *103*, 556–592. [CrossRef]
4. Mahian, O.; Kolsi, L.; Amani, M.; Estellé, P.; Ahmadi, G.; Kleinstreuer, C.; Marshall, J.S.; Taylor, R.A.; Abu-Nada, E.; Rashidi, S.; et al. Recent advances in modeling and simulation of nanofluid flows-Part II: Applications. *Phys. Rep.* **2019**, *791*, 1–59. [CrossRef]
5. El-Kaddadi, L.; Asbik, M.; Zari, N.; Zeghmati, B. Experimental study of the sensible heat storage in the water/TiO_2 nanofluid enclosed in an annular space. *Appl. Therm. Eng.* **2017**, *122*, 673–684. [CrossRef]
6. Cieśliński, J.T.; Fabrykiewicz, M. Thermal energy storage using stearic acid as PCM material. *J. Mech. Energy Eng.* **2018**, *2*, 217–224.
7. Hussein, A.M.; Sharma, K.V.; Bakar, R.A.; Kadirgama, K. A review of forced convection heat transfer enhancement and hydrodynamic characteristics of a nanofluid. *Renew. Sustain. Energy Rev.* **2014**, *29*, 734–743. [CrossRef]
8. Mahian, O.; Kolsi, L.; Amani, M.; Estellé, P.; Ahmadi, G.; Kleinstreuer, C.; Marshall, J.S.; Siavashi, M.; Taylor, R.A.; Niazmand, H.; et al. Recent advances in modeling and simulation of nanofluid flows-Part I: Fundamentals and theory. *Phys. Rep.* **2019**, *790*, 1–48. [CrossRef]
9. Haddad, Z.; Oztop, H.F.; Abu-Nada, E.; Mataoui, A. A review on natural convective heat transfer of nanofluids. *Renew. Sust. Energ. Rev.* **2012**, *16*, 5363–5378. [CrossRef]
10. Cieśliński, J.T.; Krygier, K. Free convection of water-Al_2O_3 nanofluid from horizontal porous coated tube. *Key Eng. Mater.* **2014**, *597*, 15–20. [CrossRef]
11. Kiran, M.R.; Babu, S.R. Experimental investigation on natural convection heat transfer enhancement using transformer oil-TiO_2 nano fluid. *Int. Res. J. Eng. Technol. (IRJET)* **2018**, *5*, 1412–1418.
12. Habibi, M.R.; Amini, M.; Arefmanesh, A.; Ghasemikafrudi, E. Effects of viscosity variations on buoyancy-driven flow from a horizontal circular cylinder immersed in Al_2O_3-water nanofluid. *Iran. J. Chem. Eng.* **2019**, *38*, 213–232.
13. Polidori, G.; Fohanno, S.; Nguyen, C.T. A note on heat transfer modelling of Newtonian nanofluids in laminar free convection. *Int. J. Thermal Sci.* **2007**, *46*, 739–744. [CrossRef]
14. Brinkman, H.C. The viscosity of concentrated suspensions and solutions. *J. Chem. Phys.* **1952**, *20*, 571. [CrossRef]
15. Maïga, S.E.B.; Palm, S.J.; Nguyen, C.T.; Roy, G.; Galanis, N. Heat transfer enhancement by using nanofluids in forced convection flows. *Int. J. Heat Fluid Flow* **2005**, *26*, 530–546. [CrossRef]
16. Cieśliński, J.T.; Smolen, S.; Sawicka, D. Free convection heat transfer from horizontal cylinders. *Energies* **2021**, *14*, 559. [CrossRef]
17. Fand, R.M.; Morris, E.W.; Lum, M. Natural convection heat transfer from horizontal cylinders to air, water and silicone oils for Rayleigh numbers between 3×10^2 to 2×10^7. *Int. J. Heat Mass Transf.* **1997**, *20*, 1173–1184. [CrossRef]
18. Ashjaee, M.; Yazdani, S.; Bigham, S.; Yousefi, T. Experimental and numerical investigation on free convection from a horizontal cylinder located above an adiabatic surface. *Heat Transf. Eng.* **2012**, *33*, 213–224. [CrossRef]
19. Atayılmaz, Ş.Ö.; Teke, İ. Experimental and numerical study of the natural convection from a heated horizontal cylinder. *Int. Commun. Heat Mass Transf.* **2009**, *36*, 731–738. [CrossRef]
20. Cieśliński, J.T.; Pudlik, W. Laminar free-convection from spherical segments. *Int. J. Heat Fluid Flow.* **1988**, *9*, 405–409. [CrossRef]
21. Sawicka, D.; Cieśliński, J.T.; Smoleń, S. A comparison of empirical correlations of viscosity and thermal conductivity of water-ethylene glycol-Al_2O_3 nanofluids. *Nanomaterials* **2020**, *10*, 1487. [CrossRef]
22. Pak, B.C.; Cho, Y.I. Hydrodynamic and heat transfer study of dispersed fluids with submicron metallic oxide particles. *Exp. Heat Transf.* **1998**, *11*, 151–170. [CrossRef]
23. Khanafer, K.; Vafai, K.; Lightstone, M. Buoyancy-driven heat transfer enhancement in a two-dimensional enclosure utilizing nanofluids. *Int. J. Heat Mass Transf.* **2003**, *46*, 3639–3653. [CrossRef]
24. ASHRAE. American Society of Heating, Refrigerating and Air-Conditioning Engineers. In *ASHRAE Handbook—Fundamentals*; ASHRAE: Atlanta, GA, USA, 2005.
25. Buongiorno, J.; Venerus, D.C.; Prabhat, N.; McKrell, T.J.; Townsend, J.; Christianson, R.J.; Tolmachev, Y.V.; Keblinski, P.; Hu, L.-W.; Alvarado, J.L.; et al. A benchmark study on the thermal conductivity of nanofluids. *J. Appl. Phys.* **2009**, *106*, 094312. [CrossRef]
26. Vajjha, R.S.; Das, D.K. Specific heat measurement of three nanofluids and development of new correlations. *ASME J. Heat Transf.* **2009**, *131*, 071601. [CrossRef]
27. Ho, C.J.; Liu, W.K.; Chang, Y.S.; Lin, C.C. Natural convection heat transfer of alumina–water nanofluid in vertical square enclosures: An experimental study. *Int. J. Therm. Sci.* **2010**, *49*, 1345–1353. [CrossRef]
28. Yu, W.; Xie, H. A Review on nanofluids: Preparation, stability mechanisms, and applications. *J. Nanomater.* **2012**, *2012*, 435873. [CrossRef]
29. Kouloulias, K.; Sergis, A.; Hardalupas, Y. Sedimentation in nanofluids during a natural convection experiment. *Int. J. Heat Mass Transf.* **2016**, *101*, 1193–1203. [CrossRef]

30. Fuskele, V.; Sarviya, R.M. Recent developments in nanoparticles synthesis, preparation and stability of nanofluids. *Mater. Today: Proc.* **2017**, *4*, 4049–4060. [CrossRef]
31. Churchill, S.; Chu, H. Correlating equations for laminar and turbulent free convection from a horizontal cylinder. *Int. J. Heat Mass Transf.* **1975**, *18*, 1049–1053. [CrossRef]
32. Putra, N.; Roetzel, W.; Das, S.K. Natural convection of nanofluids. *Heat Mass Transf.* **2003**, *39*, 775–784. [CrossRef]
33. Xuan, Y.; Roetzel, W. Conceptions for heat transfer correlations of nanofluids. *Int. J. Heat Mass Transf.* **2000**, *43*, 3701–3707. [CrossRef]
34. Ho, C.J.; Chen, M.W.; Li, Z.W. Numerical simulation of natural convection of nanofluid in a square enclosure: Effects due to uncertainties of viscosity and thermal conductivity. *Int. J. Heat Mass Transf.* **2008**, *51*, 4506–4516. [CrossRef]